B PHYSICS AT Belle* **

KENKICHI MIYABAYASHI

for the Belle collaboration

Department of Physics, Nara Women's University
Kita-Uoya-Nishi-machi, Nara 630-8506, Japan
e-mail: miyabaya@hepl.phys.nara-wu.ac.jp

(Received May 7, 2001)

We present recent results on B physics from the Belle detector at the KEKB asymmetric e^+e^- collider. The mixing-induced CP violation parameter is measured to be $\sin 2\phi_1 = 0.58^{+0.32}_{-0.34}(\text{stat.})^{+0.09}_{-0.10}(\text{syst.})$ based on a data sample of 10.5 fb^{-1} at the $\Upsilon(4S)$ resonance. Other topics including B–$\bar{B}$ mixing, observations of rare decays, and $|V_{cb}|$ measurements are also reported.

PACS numbers: 11.30.Er, 12.15.Hh, 13.20.He, 13.25.Hw

1. Introduction

The study of CP violation in B meson decay is one of the key tests of the Standard Model (SM). The existence of a complex phase causes CP violating phenomena, and is thought to originate in the quark mixing matrix which is called the Cabbibo–Kobayashi–Maskawa (CKM) matrix [1]. The CKM matrix is written as [2];

$$\begin{pmatrix} V_{ud} & V_{us} & V_{ub} \\ V_{cd} & V_{cs} & V_{cb} \\ V_{td} & V_{ts} & V_{tb} \end{pmatrix} = \begin{pmatrix} 1-\lambda^2/2 & \lambda & A\lambda^3(\rho - i\eta) \\ -\lambda & 1-\lambda^2/2 & A\lambda^2 \\ A\lambda^3(1-\rho-i\eta) & -A\lambda^2 & 1 \end{pmatrix}, \tag{1}$$

* Presented at the Cracow Epiphany Conference on b Physics and CP Violation, Cracow, Poland, January 5–7, 2001.

** Talk slides can be found at: http://www.hepl.phys.nara-wu.ac.jp/~miyabaya/krakow2001/epiphany.htm.

where V_{ub} and V_{td} have CP violating complex phases. Due to the unitarity condition of CKM matrix, the following relation is expected to hold.

$$V_{td}V_{tb}^* + V_{cd}V_{cb}^* + V_{ud}V_{ub}^* = 0\,. \tag{2}$$

Here, the CP violating angles ϕ_1, ϕ_2 and ϕ_3 are defined as shown in Fig. 1.

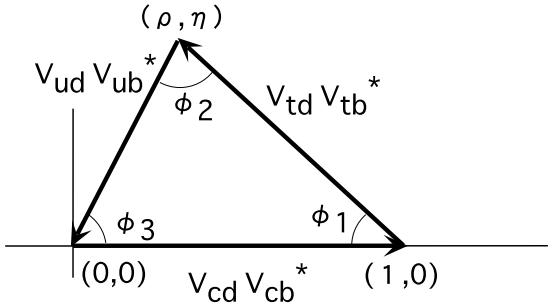

Fig. 1. The unitarity triangle. The CP violation parameters are defined as the angles of ϕ_1, ϕ_2 and ϕ_3.

Since all terms in Eq. (2) have the same order, the angles of this triangle are expected to be as large as $\sim O(0.1)$ resulting in large CP asymmetries.

B meson decays can be used to measure the CP violating angles ϕ_1, ϕ_2 and ϕ_3 and the lengths of the sides of this triangle. With four measurements, this allows us to make a comprehensive test of the CKM scheme by overconstraining this triangle.

There are two categories of CP violation phenomena; indirect and direct CP violation. The former is induced by B^0–$\bar{B}^0$ mixing while the latter is due to the interference of two decay amplitudes.

Among these categories, the most promising one is indirect CP violation which leads to a time-dependent CP asymmetry which directly accesses $\sin 2\phi_1$. In order to observe it, the following requirements have to be satisfied: CP eigenstates must be efficiently reconstructed with high purity, the B meson flavor must be identified and the B meson's proper time t must be measured with good resolution.

The solution is a high intensity e^+e^- asymmetric collider on the $\Upsilon(4S)$ resonance and a general purpose spectrometer having good vertex, energy and momentum resolution together with high momentum particle identification capability. We call this facility a B-factory. At the *High Energy Accelerator Research Organization* (KEK), the KEKB accelerator and the Belle detector are working together as a B-factory.

2. Experimental apparatus

The KEKB accelerator collides 3.5 GeV e^+ with 8 GeV e^-. The beams are stored separately in a High Energy Ring (HER; e^-) and a Low Energy Ring (LER; e^+) having a 3 km circumference. The beams cross at an angle of 22 mrad at the interaction point. The produced $\Upsilon(4S)$ system is boosted with $\beta\gamma = 0.425$ in the laboratory frame so that the B mesons then travel approximately 200 μm during their mean life.

After observation of the first collision events in June 1999, the luminosity has been gradually increasing. As shown in Fig. 2, the luminosity has steadily improved from April 2000. By the end of 2000, a total of 11 fb^{-1} was accumulated. Colliding beam operation resumed in February 2001 with typical peak and daily integrated luminosities of 3×10^{33} cm^{-2}s^{-1} and ~ 200 pb^{-1}/day, respectively.

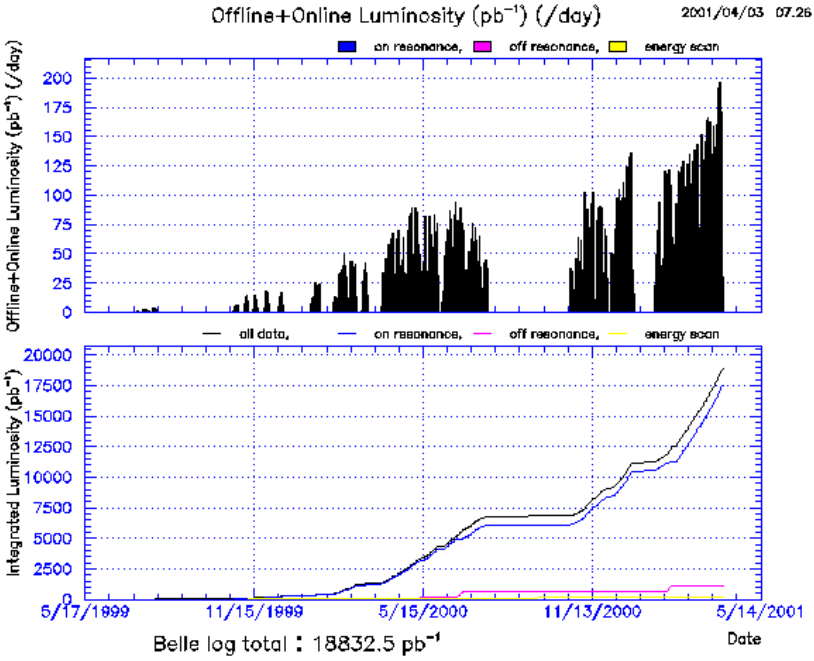

Fig. 2. Achievements of KEKB accelerator operation. The upper plot is integrated luminosity in units of pb^{-1}/day, while the lower plot is total integrated luminosity. Both are plotted as the function of date. 18 fb^{-1} was accumulated in total by the end of March 2001.

A detailed description of the Belle detector can be found elsewhere [3]. It consists of a three-layer Silicon Vertex Detector (SVD), a Central Drift Chamber (CDC) filled with a normal pressure helium–ethane mixture

(H_e : C_2H_6 = 50 : 50), an array of Aerogel Čerenkov Counters (ACC), Time-Of-Flight scintillation counters (TOF), an Electromagnetic Calorimeter using 8736 CsI(Tl) crystals (ECL), 1.5 T super-conducting solenoid, and 14 layers of iron flux-return yoke interleaved with resistive plate counters (KLM).

The momentum resolution for charged particles is

$$\left(\frac{\sigma_{p_T}}{p_T}\right)^2 = (0.0019 p_T)^2 + (0.0034)^2 ,$$

where p_T is the transverse momentum with respect to the beam axis in units of GeV/c. The impact parameter resolutions are $\sigma_{r\phi} \sim \sigma_z = 55$ μm for $p = 1$ GeV/c tracks at normal incidence. Charged particles are identified by specific ionization (dE/dx) measurements in the CDC ($\sigma_{dE/dx} = 6.9$ %), TOF flight-time measurements ($\sigma_{TOF} = 95$ ps) and the number of photoelectrons detected in ACC. Charged kaon identification is performed in the momentum range up to 3.5 GeV/c with an efficiency of 85 % and a 10 % charged pion fake rate. For electron identification, the ratio between the charged track's momentum and the associated shower energy (E/p) is the most powerful observable. Other information including dE/dx, the distance between the ECL shower and the extrapolated track, and the shower shape are also used. The efficiency is greater than 90 % and the hadron fake rate is less than 0.3 %. Muons are identified by requiring the association between KLM hits and an extrapolated track. The efficiency is more than 90 % while the fake rate is less than 3 %. The energy resolution of the ECL for photons is $(\sigma_E/E)^2 = (0.013)^2 + (0.0007/E)^2 + (0.008/E^{1/4})^2$, where E is in GeV. K_L mesons are detected by KLM hits together with ECL information. An angular resolution better than 3° is achieved for K_L mesons.

3. Measurement of sin 2ϕ_1

The SM predicts large CP violation in the difference of the time-dependent decay rates between B^0 and $\bar{B}^0$ into a common CP eigenstate, f_{CP}. When the decays into f_{CP} take place predominantly by one amplitude having no complex phase, interference with B^0–$\bar{B}^0$ mixing causes a CP asymmetry, $A_{CP}(t)$, which directly accesses the angle ϕ_1.

$$A_{CP}(t) \equiv \frac{R(\bar{B}^0 \to f_{CP}) - R(B^0 \to f_{CP})}{R(\bar{B}^0 \to f_{CP}) + R(B^0 \to f_{CP})} = -\xi_{CP} \sin 2\phi_1 \sin \Delta m_d t , \quad (3)$$

where $R(\bar{B}^0(B^0) \to f_{CP})$ is the decay rate for a $\bar{B}^0(B^0)$ to f_{CP} at a proper time t after production, ξ_{CP} is CP the eigenvalue of f_{CP}, Δm_d is the mass

difference between the two mass eigenstates, and ϕ_1 is one of the angles of the unitarity triangle defined as $\phi_1 \equiv \pi - \arg\left(\frac{-V_{tb}^* V_{td}}{-V_{cb}^* V_{cd}}\right)$, which is also shown in Fig. 1.

The B^0–$\bar{B}^0$ pair from $\Upsilon(4S)$ is in a coherent p-wave state until one of them decays. Therefore, at the moment when one B meson decays into the state ($f_{\rm tag}$) telling whether it is B^0 or $\bar{B}^0$, at a time $t_{\rm tag}$, the other one is definitely of the opposite flavor. The remaining one decays into f_{CP} at a time t_{CP}. Here, because of the coherent oscillation of B meson pairs from $\Upsilon(4S)$ before one of them decays, the proper time t should be taken as the proper time difference, $\Delta t \equiv t_{CP} - t_{\rm tag}$.

CP eigenstates $J/\psi K_{\rm S}$, $\psi' K_{\rm S}$, $\chi_{c1} K_{\rm S}$, $\eta_c K_{\rm S}$, $J/\psi K_{\rm L}$ and $J/\psi\pi^0$ are used in this analysis. Among these, $J/\psi K_{\rm L}$ and $J/\psi\pi^0$ have $\xi_{CP} = +1$ while all other modes have $\xi_{CP} = -1$.

J/ψ mesons are reconstructed in $l^+l^-(l = e, \mu)$ decay modes. In the e^+e^- case, the naive invariant mass of two tracks has a long tail because of bremsstrahlung from the final state electron or positron. In order to recover as much of this tail as possible, ECL showers found within 50 mrad from the track's initial direction are included to calculate the invariant mass ($M_{ee(\gamma)}$). Candidates in the $\mu^+\mu^-$ mode are selected by cutting on the invariant mass of dimuon tracks ($M_{\mu\mu}$) because the radiative tail is much smaller. The requirements of

$$-12.5\sigma < (M_{J/\psi} - M_{ee(\gamma)}) < +3\sigma$$

and

$$-5\sigma < (M_{J/\psi} - M_{\mu\mu}) < +3\sigma$$

are used for e^+e^- and $\mu^+\mu^-$ modes, respectively, where $\sigma = 12$ MeV/c^2 is the mass resolution. For the $B^0 \to J/\psi K_{\rm S}(\pi^+\pi^-)$ mode, the requirement of lepton-identification for one of the tracks is relaxed, because this mode has a smaller background than others.

The ψ' is reconstructed by its decays into l^+l^- and $J/\psi\pi^+\pi^-$. The first mode is the same as J/ψ, and the second is reconstructed by requiring the mass difference, $m_{l^+l^-\pi^+\pi^-} - m_{l^+l^-}$, to be between 0.58 and 0.60 GeV/c^2.

χ_{c1} reconstruction is done using the $\chi_{c1} \to J/\psi\gamma$ mode. Since most photons in hadronic events come from π^0s, if a photon is combined with any other photon and the invariant mass of the two photons are consistent with M_{π^0}, the photon is rejected as a χ_{c1} candidate. Two η_c decay modes, $\eta_c \to K_{\rm S} K^\pm\pi^\pm$ and $\eta_c \to K^+K^-\pi^0$ are used to reconstruct $B^0 \to \eta_c K_{\rm S}$.

$K_{\rm S} \to \pi^+\pi^-$ candidates are selected as oppositely charged track pairs having an invariant mass within $\pm 4\sigma$ of M_{K^0}, where $\sigma \sim 4$MeV/c^2. In the $B^0 \to J/\psi K_{\rm S}$ mode, $K_{\rm S} \to \pi^0\pi^0$ decays are also used. Two $\gamma\gamma$ pairs with an invariant mass between 80 and 150 MeV/c^2 which are assumed to originate

from the interaction point are selected and the sum of the χ^2 from each π^0 mass constrained fit is minimized by varying the decay point of K_S.

For the $J/\psi\pi^0$ mode, we use a minimum photon energy of 100 MeV and select $\gamma\gamma$ pairs having an invariant mass between 118 and 150 MeV/c^2. The π^0 momentum is obtained by a mass constrained fit.

These exclusive decay channels are identified by two observables in the $\Upsilon(4S)$ center of mass (cms) frame; the beam-energy constrained mass $M_{bc} \equiv \sqrt{E_{\rm beam}^2 - (\sum \vec{p}_i)^2}$ and the energy difference $\Delta E \equiv \sum E_i - E_{\rm beam}$, where $E_{\rm beam} = \sqrt{s}/2$ is the beam energy in the cms frame, and $\vec{p}_i$ and E_i are the cms three momenta and energies of the candidate B meson decay products. M_{bc} and ΔE should be consistent with the B meson mass and zero respectively with resolutions depending on the decay mode. The M_{bc} distribution of the decay modes described above is shown in Fig. 3.

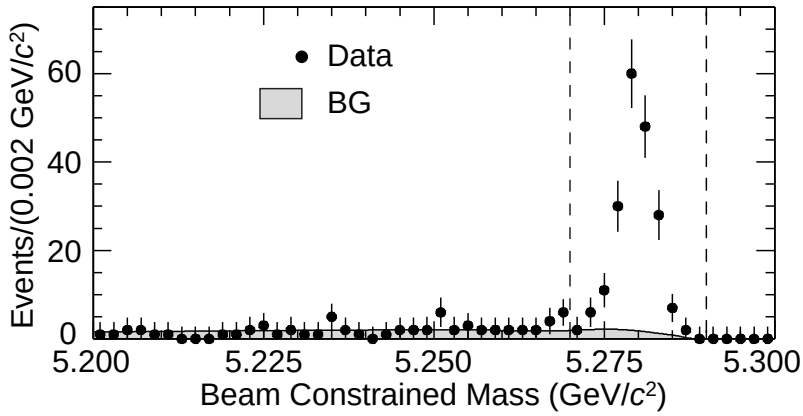

Fig. 3. The beam-constrained mass distribution for all decay modes combined other than $J/\psi K_L$. The shaded area is the estimated background. The dashed lines indicate the signal region.

$B^0 \to J/\psi K_L$ decays are selected by requiring that the observed K_L direction is within 45° from the expected direction derived from two-body decay kinematics. This constrains $p_B^{\rm cms}$, the reconstructed momentum of the B meson in the cms frame, to lie in the range $0.2 < p_B^{\rm cms} < 0.45$ GeV/c. To reduce backgrounds further, the J/ψ cms momentum, the angle between the K_L and its nearest-neighbor charged track, the charged track multiplicity and the kinematics assuming that a three-body decay hypothesis of $B^+ \to J/\psi K^{*+}(K_L\pi^+)$ are used to calculate a likelihood quantity. The $p_B^{\rm cms}$ distribution fit gives 77 $J/\psi K_L$ events out of 131 entries in the signal region. The reconstructed CP eigenstate events are summarized in Table I.

TABLE I

The numbers of CP eigenstate events. $N_{\rm EV}$ and $N_{\rm BG}$ denote number of observed events and estimated background, respectively.

Mode	$N_{\rm EV}$	$N_{\rm BG}$
$J/\psi(l^+l^-)K_{\rm S}(\pi^+\pi^-)$	123	3.7
$J/\psi(l^+l^-)K_{\rm S}(\pi^0\pi^0)$	19	2.5
$\psi'(l^+l^-)K_{\rm S}(\pi^+\pi^-)$	13	0.3
$\psi'(J/\psi\pi^+\pi^-)K_{\rm S}(\pi^+\pi^-)$	11	0.3
$\chi_{c1}(\gamma J/\psi)K_{\rm S}(\pi^+\pi^-)$	3	0.5
$\eta_c(K^+K^-\pi^0)K_{\rm S}(\pi^+\pi^-)$	10	2.4
$\eta_c(K_{\rm S}K^+\pi^-)K_{\rm S}(\pi^+\pi^-)$	5	0.4
$J/\psi(l^+l^-)\pi^0$	10	0.9
Sub-total	194	11
$J/\psi(l^+l^-)K_{\rm L}$	131	54

The flavor of the other B meson is tagged by leptons and charged kaons and pions which are not included in f_{CP}. Tracks are selected in the following categories which distinguish the b-flavor by the track's charge; high momentum leptons from $b \to cl^-\bar{\nu}$, slow leptons from $c \to sl^+\nu$, charged kaons from $b \to c \to s$, high momentum pions coming from the decays of $B^0 \to D^{(*)-}(\pi^+, \rho^+, a_1^+,\ etc.)$ and slow pions from $D^{*-} \to \bar{D}^0\pi^-$. For each category, we determined the relative probability density to give b-flavor information by MC. Taking the correlation among different categories into account, a likelihood is calculated to distinguish between B^0 and $\bar{B}^0$ and to give the flavor-tagging dilution probability on an event-by-event bases.

The probability to give an incorrect flavor, which is called the wrong tag fraction w, is directly checked in data using the self-tagging final states $B^0 \to D^{*-}l^+\nu, D^{(*)-}\pi^+$, and $D^{*-}\rho^+$. Applying the flavor-tagging logic to the other B meson, we can estimate w from the time dependent opposite–same flavor asymmetry, $A_F(t)$ becomes; $A_F(t) = (1-2w)\cos(\Delta m_d t)$. The overall tagging efficiency ε is found to be 99.6 % and the total effective efficiency $\varepsilon_{\rm eff} \equiv \varepsilon(1-2w)^2$ is estimated to be $27.0^{+2.1}_{-2.2}$ %.

The vertex positions for f_{CP} and $f_{\rm tag}$ are reconstructed using tracks having associated hits in the SVD. Each vertex position is required to be consistent with the run-dependent IP profile in the $r\phi$ plane. The typical IP size is $\sigma_x \sim 100$ μm, $\sigma_y \sim 5$ μm and $\sigma_z \sim 3$ mm. The f_{CP} vertex is determined by lepton tracks from the J/ψ or ψ' decays, or prompt tracks coming from η_c. The $f_{\rm tag}$ vertex is determined from tracks not assigned to

f_{CP}. According to MC studies, the vertex resolutions in the z direction for f_{CP} and $f_{\rm tag}$ are 75 μm and 140 μm, respectively. The poorer resolution for $f_{\rm tag}$ is due to the lower average momentum of the $f_{\rm tag}$ decay products and the smearing by the charmed meson lifetime. The resolution function $R(\Delta t)$ for the proper time difference is parameterized as a sum of two Gaussian components. The estimated error of Δt is given on an event-by-event basis. In order to test the validity of the resolution function, B meson lifetimes are measured by non-CP modes;

$$B^0 \to J/\psi K^{*0}, \quad D^{(*)-}\pi^+(\rho^+), \quad D^{*-}l^+\nu$$

and

$$B^+ \to J/\psi K^+, \quad D^0\pi^+, \quad D^{*0}l^+\nu\,.$$

The results are $\tau_{B^0} = 1.548 \pm 0.03 \pm 0.07$ ps and $\tau_{B^+} = 1.67 \pm 0.04^{+0.11}_{-0.10}$ ps, where the first error is statistical and the second error is systematic. These are consistent with the PDG values [4].

The CP violating parameter, $\sin 2\phi_1$ is determined from an unbinned maximum likelihood fit to the observed Δt distributions. The probability density function (pdf) for the signal distribution is given by

$$P_{\rm SIG}(\Delta t) - \frac{{\rm e}^{-|\Delta t|/\tau_{B^0}}}{2\tau_{B^0}}[1 - \xi_{CP}\, q(1-2w)\sin 2\phi_1 \sin(\Delta m_d \Delta t)]\,, \qquad (4)$$

where q denotes the B flavor ($+1$ for B^0 and -1 for $\bar{B}^0$) and τ_{B^0} and Δm_d are fixed at their world average values. The pdf for background events is parameterized as $P_{\rm BG}(\Delta t) = f_\tau {\rm e}^{-|\Delta t|/\tau_{\rm BG}}/2\tau_{\rm BG} + (1-f_\tau)\delta(\Delta t)$. The pdfs are convoluted with $R(\Delta t)$ to construct the likelihood value for each event as a function of $\sin 2\phi_1$:

$$L_i = \int \left[f_{\rm SIG} P_{\rm SIG}(\Delta t') + (1-f_{\rm SIG}) P_{\rm BG}(\Delta t')\right] R(\Delta t - \Delta t') d\Delta t', \qquad (5)$$

where $f_{\rm SIG}$ is the probability that the event is a signal calculated from $p_B^{\rm cms}$ for $J/\psi K_{\rm L}$, and from ΔE and M_{bc} for other modes. The most probable $\sin 2\phi_1$ is the value which maximizes the likelihood function $L = \sum L_i$. The obtained value is:

$$\sin 2\phi_1 = 0.58^{+0.32}_{-0.34}({\rm stat.})^{+0.09}_{-0.10}({\rm syst.})\,. \qquad (6)$$

The asymmetry in each Δt bin is shown in Fig. 4 together with the curve corresponding to the global fit result [5].

In order to check a possible bias, the same fitting procedure was applied to non-CP eigenstate modes of $B^0 \to D^{(*)-}\pi^+$, $D^{*-}\rho^+$, $J/\psi K^{*0}(K^+\pi^-)$, $D^{*-}l^+\nu$ and $B^+ \to J/\psi K^+$. For all the modes combined, the asymmetry is 0.065 ± 0.075, which is consistent with zero.

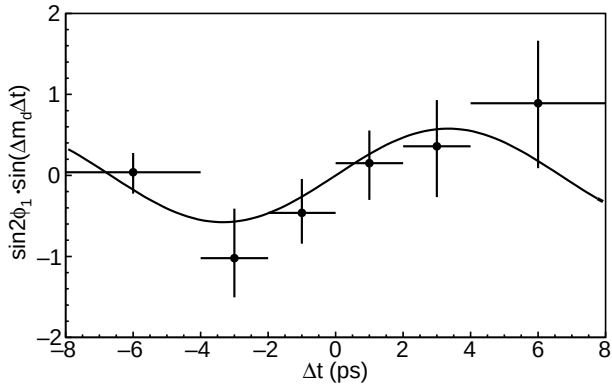

Fig. 4. The asymmetry obtained from separate fits to each Δt bin. The curve is the result of the global fit ($\sin 2\phi_1 = 0.58$).

4. Other charmonium involving decays

Some B meson decays into charmonia, in addition to the modes already used for the $\sin 2\phi_1$ measurement, could be used to study CP violating phenomena. Here, the decays into $J/\psi K^*$ and $J/\psi K_1$ are discussed.

4.1. Polarization measurement of J/ψ in $B \to J/\psi K^*$

The measurement of the polarization of the J/ψ in $B \to J/\psi K^*$ decays is a good test of the factorization hypothesis [6]. Due to the nature of the decay of a pseudo-scalar into two vector mesons, the angular-momentum between the final state mesons is a linear combination of s, p and d-waves, *i.e.* CP even and odd states are mixed. The measurement of the J/ψ polarization gives information on the amount of the mixture. There are three complex amplitudes A_0, $A_{\|}$ and $A_{\perp}$ corresponding to three helicity states of $J/\psi K^*$. $A_{\perp}$ is the CP odd component for the case of $J/\psi(K_S\pi^0)^{*0}$. The two remaining amplitudes give the CP even contribution. $|A_0|^2$ is the fraction with longitudinal polarization of the J/ψ. These amplitudes are normalized as $|A_0|^2 + |A_{\|}|^2 + |A_{\perp}|^2 = 1$. These amplitudes are determined by a fit to the angular distribution of the decay products from J/ψ and K^*.

In order to perform this angular analysis, the decay modes $B^+ \to J/\psi K^{*+}$ ($K^{*+} \to K_S\pi^+$) are used. The methods used to reconstruct the J/ψ and K_S are the same as those used for the CP modes in the $\sin 2\phi_1$ measurement. Charged kaons are selected by requiring that the probability of kaon hypothesis is greater than 0.4. Signal yields in data sample for each decay modes are listed in Table II, with small amount of backgrounds; 5.9 % for $B^0 \to J/\psi K^{*0}(K^{*0} \to K^+\pi^-)$ and 10.8 % for $B^+ \to J/\psi K^{*+}(K^{*+} \to K_S\pi^+)$.

TABLE II

Signal yields of $J/\psi K^*$ modes used for the angular analysis in the data sample.

Mode	Yield
$J/\psi(l^+l^-)(K^+\pi^-)^{*0}$	273
$J/\psi(l^+l^-)(K_S\pi^+)^{*+}$	56

Combining the two decay modes, fitting to angular distributions of final state particles gives the results: $|A_0|^2 = 0.54 \pm 0.04 \pm 0.04$, $|A_\perp|^2 = 0.20 \pm 0.05 \pm 0.04$, $\arg(A_\parallel) = 3.10 \pm 0.31 \pm 0.07$ and $\arg(A_\perp) = 0.00 \pm 0.25 \pm 0.03$, where the first error is statistical and second is systematic. Our polarization measurement is consistent with previous measurements [7].

4.2. Observation of $B \to J/\psi K_1$

Although the branching fraction for inclusive $B \to J/\psi X$ decay is relatively large, only a small fraction of exclusive modes which are contained in the inclusive signal are useful for CP studies. Therefore, it is interesting to search for additional decay modes which could be used in a CP analysis. In addition, the inclusive J/ψ spectrum is not saturated by summing up the exclusive decay modes which are presently observed. Therefore, finding new decay modes could provide a better understanding of charmonium production from B meson decays.

Decays of the type $B^0 \to J/\psi K_1^0(1270)$ are of interest because the $K_1^0(1270)$ has an appreciable branching fraction to the flavor-nonspecific $K^0\rho^0$ final state (14 %). Therefore, $B \to J/\psi K\pi\pi$ decays are studied with three final state topologies: $B^+ \to J/\psi K^+\pi^+\pi^-$, $B^0 \to J/\psi K^+\pi^-\pi^0$ and $J/\psi K^0\pi^+\pi^-$, where $K^0 \to \pi^+\pi^-$. The observed invariant mass spectrum of $K\pi\pi$ is consistent with that of the $K_1(1270)$ resonance, and the signal yields obtained are summarized in Table III.

TABLE III

Signal yields of $J/\psi K\pi\pi$ modes and $J/\psi K^+$.

Mode	Yield
$J/\psi K^+\pi^+\pi^-$	53.4±9.1
$J/\psi K^+\pi^-\pi^0$	19.3±5.1
$J/\psi K^0\pi^+\pi^-$	6.2±2.6
$J/\psi K^+$	472.4±22.9

These results are normalized to the $B^+ \to J/\psi K^+$ decay mode, and the relative branching fractions which are obtained are translated into absolute ones:

$$\mathcal{B}(B^0 \to J/\psi K_1^0(1270)) = (1.30 \pm 0.34 \pm 0.31) \times 10^{-3}$$

and

$$\mathcal{B}(B^+ \to J/\psi K_1^+(1270)) = (1.80 \pm 0.34 \pm 0.39) \times 10^{-3}\,,$$

where the first error is statistical and the second is systematic.

5. B–$\bar{B}$ mixing measurement with dilepton events

The frequency of B^0–$\bar{B}^0$ mixing is proportional to the mass difference between the two mass eigenstates of neutral B meson, Δm_d which is a fundamental parameter of the B system. At the $\Upsilon(4S)$, the asymmetry in the time evolution between same-flavor (B^0B^0 or $\bar{B}^0\bar{B}^0$) and opposite-flavor ($B^0\bar{B}^0$) decays exhibits an oscillation as a function of the proper time difference between the two B meson decays, Δt, with a frequency that is proportional to Δm_d. Both the B flavor tag and the decay vertex position can be determined with high-momentum leptons. Here, we report a study of B–$\bar{B}$ mixing with dilepton events based on integrated luminosities of 5.9 fb^{-1} at the $\Upsilon(4S)$ resonance and 0.6 fb^{-1} at an energy 60 MeV below the peak.

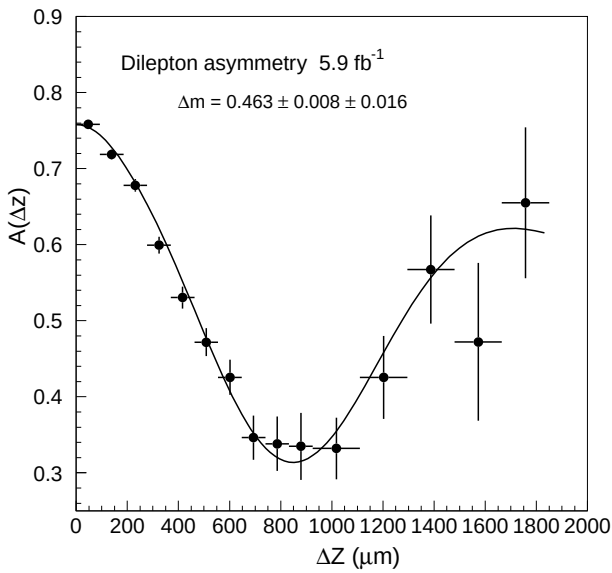

Fig. 5. Opposite and same-sign dilepton asymmetry *vs* Δz. The points are data. The curve is the result of the fit.

On the $\Upsilon(4S)$, 8573 Same-Sign (SS) and 40981 Opposite-Sign (OS) dilepton events are observed, and 40 SS and 198 OS dileptons are found below the resonance. Each dilepton event belongs to one of three classes: signal (S), correctly tagged background (C), or incorrectly tagged background (W). The detection efficiency and background contribution are determined with MC.

To extract Δm_d, a binned maximum likelihood fit is performed simultaneously to the Δz distributions of the SS and OS dileptons. Fig. 5 shows the OS and SS asymmetry, $(N_{\rm OS} - N_{\rm SS})/(N_{\rm OS} + N_{\rm SS})$, for data together with the result of the fit [8]. We obtain

$$\Delta m_d = 0.463 \pm 0.008(\text{stat.}) \pm 0.016(\text{syst.})\ \text{ps}^{-1} \tag{7}$$

which is consistent with the world average value [4].

6. Study on $b \to s$ penguin transitions

The $b \to s$ penguin transitions are mediated by virtual W bosons in the SM. These transitions are of interest because non-SM particles, such as charged Higgs bosons or supersymmetric particles, can also contribute in the loops and potentially produce deviations from SM expectations. Here, we report results on the radiative $b \to s\gamma$ decay, which is caused by an electroweak penguin diagram and $B \to \phi K$ modes, which result from a hadronic penguin contribution.

6.1. The $b \to s\gamma$ decay

The radiative $b \to s\gamma$ transition is observed as the inclusive decay $B \to X_s\gamma$, where X_s denotes a hadronic recoil system containing an s quark. The signature of this process is a high energy photon accompanied by a kaon. The recoil system X_s is reconstructed in 16 different final states from one charged kaon or $K_{\rm S}$ plus one to four pions which may include one π^0. The primary photon is combined with every X_s and the opening angle $\theta_{X_s\gamma}$ between $\vec{p_\gamma}$ and $\vec{p_{X_s}}$, ΔE and M_{bc} are calculated in the cms frame. We require $\theta_{X_s\gamma} > 167^\circ$, $M_{bc} > 5.2$ GeV/c^2 and $-0.15 < \Delta E/\text{GeV} < 0.10$ to select $B \to X_s\gamma$ candidates. When multiple candidates are found in an event, the best candidate is selected using vertex information and $\theta_{X_s\gamma}$. After the best candidate is found, we required $M_{X_s} < 2.05$ GeV/c^2. Background comes mainly from continuum $q\bar{q}$ production where the hard photon originates from initial state radiation or from a high momentum π^0 or η with an undetected photon. A Fisher discriminant calculated from a set of event variables is used to select a background enhanced sample and to model the background shape. We obtain a branching fraction of $B \to X_s\gamma$:

$$\mathcal{B}(B \to X_s\gamma) = (3.36 \pm 0.53 \pm 0.42^{+0.50}_{-0.54}) \times 10^{-4}, \tag{8}$$

where the first error is statistical, the second is systematic and the third is the theoretical model error [9]. Our result is consistent with the SM prediction [10] and previous measurements by the CLEO and ALEPH experiments [11].

6.2. Observation of $B \to \phi K^{(*)}$ decays

Decays such as $B \to \phi K$ cannot take place via a tree diagram and are expected to be dominated by the $b \to s s\bar{s}$ penguin diagram. The ϕ mesons are reconstructed in the K^+K^- final state from oppositely charged track pairs, in which each track is consistent with the kaon hypothesis and which satisfy $|M_{KK} - M_\phi| < 10$ MeV/c^2. The modes used to detect K_S and K^* mesons are the same as in Sections 3 and 4.1. Among all the modes that were searched for, only the $B^+ \to \phi K^+$ mode had a significant excess. The significance of the signal is 7.6σ and the branching fraction is measured to be $\mathcal{B}(B^+ \to \phi K^+) = (1.39^{+0.32}_{-0.30}(\text{stat.}) \pm 0.25(\text{syst.})) \times 10^{-5}$.

7. Rare decays to access ϕ_2 and ϕ_3

The $B \to D^{(*)}K^{(*)}$ modes play an important role in the measurement of the angle ϕ_3 via direct CP violation. The charmless hadronic B decays $B \to \pi\pi, K\pi$ and KK are also interesting since indirect and direct CP violation in these modes are related to the angles ϕ_2 and ϕ_3.

7.1. The $D^{(*)}K$ decays

The theoretically cleanest way to determine ϕ_3 is by observation of a CP asymmetry induced by the interference between $b \to c$ and $b \to u$ transition amplitudes in the Cabibbo-suppressed $B^- \to D^0 K^-$ decay channel. First of all, it is necessary to establish the existence of the Cabibbo-suppressed modes. Since the Cabibbo-favored $D^{(*)}\pi$ decays have quite similar kinematics, the signal yields for $D^{(*)}K$ and $D^{(*)}\pi$ are simultaneously calculated by fitting ΔE after dividing the data into a $D^{(*)}\pi$ dominant sample and a $D^{(*)}K$ enriched sample on the basis of kaon probability for the charged hadron accompanying $D^{(*)}$. The cut is at a probability of 0.8. Because of the difference between the masses of the kaon and pion, the $D^{(*)}K$ peak is shifted to $\Delta E = -49$ MeV. The ratios of Cabibbo-suppressed to Cabibbo-favored branching fractions are found to be:

$$\frac{\mathcal{B}(B^- \to D^0 K^-)}{\mathcal{B}(B^- \to D^0 \pi^-)} = 0.077 \pm 0.0009 \pm 0.006\,,$$

$$\frac{\mathcal{B}(\bar{B}^0 \to D^+ K^-)}{\mathcal{B}(\bar{B}^0 \to D^+ \pi^-)} = 0.066 \pm 0.0015 \pm 0.007\,,$$

$$\frac{\mathcal{B}(B^- \to D^{*0}K^-)}{\mathcal{B}(B^- \to D^{*0}\pi^-)} = 0.076 \pm 0.0019 \pm 0.009\,,$$
$$\frac{\mathcal{B}(\bar{B}^0 \to D^{*+}K^-)}{\mathcal{B}(\bar{B}^0 \to D^{*+}\pi^-)} = 0.072 \pm 0.0015 \pm 0.006\,. \quad (9)$$

The first error is statistical and the second is systematic. These are first reported observations of the $B \to D^+K^-, D^{*0}K^-$ and $D^{*+}K^-$ decay processes.

7.2. The two body $\pi\pi, \pi K$ and KK decay modes

We studied charmless hadronic two-body B decays into $\pi\pi$, $K\pi$ and KK final states. The charge combinations studied are $\pi^+\pi^-$, $K^+\pi^-$, K^+K^-, $K^0\pi^0$ for B^0 decays and $\pi^+\pi^0$, $K^+\pi^0$ $K^0\pi^+$ $K^+\bar{K}^0$ for B^+ decays. For the modes with K^0 mesons, K_S mesons are reconstructed only by their decays into $\pi^+\pi^-$. After applying event shape based selection criteria for further background rejection, the M_{bc} and ΔE distributions of the remaining sample are used: the shape of the background is modeled by sideband data, then because of the kinematic separation between $h\pi^+$ and hK^+ decays, the results of the ΔE fit are used to determine the signal yields. The results are summarized in Table IV.

TABLE IV

Signal yields and branching fractions of hadronic two-body B decays.

Mode	Yield	Significance	Branching fraction($\times 10^{-5}$)
$B^0 \to \pi^+\pi^-$	$17.7^{+7.1+0.3}_{-0.3-1.1}$	3.1	$0.56^{+0.23}_{-0.20} \pm 0.04$
$B^+ \to \pi^+\pi^0$	$10.4^{+5.1+1.2}_{-4.3-4.3}$	2.7	$0.78^{+0.38+0.08}_{-0.32-0.12}$ (< 1.34 at 90 % C.L.)
$B^0 \to K^+\pi^-$	$60.3^{+10.6+2.7}_{-9.9\ -1.1}$	7.8	$1.93^{+0.34+0.15}_{-0.32-0.06}$
$B^+ \to K^+\pi^0$	$34.9^{+7.6+0.6}_{-7.0-2.0}$	7.2	$1.63^{+0.35+0.16}_{-0.33-0.18}$
$B^+ \to K^0\pi^+$	$10.3^{+4.3+0.4}_{-3.6-0.1}$	3.5	$1.37^{+0.57+0.19}_{-0.48-0.18}$
$B^0 \to K^0\pi^0$	$8.4^{+3.8+0.4}_{-3.1-0.6}$	3.9	$1.60^{+0.72+0.25}_{-0.59-0.27}$
$B^0 \to K^+K^-$	$0.2^{+3.8}_{-0.2}$	—	—
$B^+ \to K^+\bar{K}^0$	$0.0^{+0.9}_{-0.0}$	—	—

8. CKM elements measurement

The measurement of CKM matrix elements are important to overconstrain the unitarity triangle. Here, studies on semileptonic decays to obtain $|V_{cb}|$ and $B \to D_s\pi$ and $D_s\rho$ for $|V_{ub}|$ are reported.

8.1. $B \to D^* l\nu, Dl\nu$ decays to measure $|V_{cb}|$

Thanks to the recent development of Heavy Quark Effective Theory (HQET) [12], we have an expression for the $B \to D^{(*)} l\nu$ decay rates with controllable theoretical uncertainty at zero recoil of $D^{(*)}$ mesons with respect to the mother B meson. We analyze the $\bar{B}^0 \to D^+ l^- \nu$ and the $\bar{B}^0 \to D^{*+} l^- \nu$ decay modes, with $D^+ \to K^-\pi^+\pi^+$ and $D^{*+} \to D^0\pi^+$ followed by $D^0 \to K^-\pi^+$. The neutrino is reconstructed from the missing mass. The recoil is expressed as $y \equiv \vec{v}_B \cdot \vec{v}_{D^{(*)}}$ and the y distribution is fitted to obtain the decay rate at $y = 1$ corresponding to zero recoil. We obtained $|V_{cb}| = (3.91 \pm 0.12(\text{stat.}) \pm 0.15(\text{syst.}) \pm 0.16(\text{theory})) \times 10^{-2}$ in the $\bar{B}^0 \to D^{*+} l^- \nu$ decay mode and $|V_{cb}| = (4.42 \pm 0.48(\text{stat.}) \pm 0.35(\text{syst.}) \pm 0.30(\text{theory})) \times 10^{-2}$ in the $\bar{B}^0 \to D^+ l^- \nu$ mode.

8.2. Search for $B \to D_s\pi$ and $D_s\rho$

It is also possible to access $|V_{ub}|$ in $B \to D_s\pi$ and $D_s\rho$ decays, where the tree diagram contribution is expected to be dominant. Candidate D_s mesons are reconstructed in the $\phi\pi^+$, $\bar{K}^{*0}K^+$ and $K_S K^+$ final states. No significant signal is observed. Upper limits on the branching fractions are given as $\mathcal{B}(B \to D_s\pi) \leq 2.0 \times 10^{-4}$ and $\mathcal{B}(B \to D_s\rho) \leq 4.3 \times 10^{-4}$ at 90 % CL.

9. Conclusion and prospect

KEKB luminosity is improving rapidly as the betatron-tune is optimized, solenoid windings to suppress beam blow-up due to the photoelectron instability are added and a sophisticated tuning scheme of various accelerator parameters is implemented. A peak luminosity of 3×10^{33} cm^{-2} sec^{-1}, an integrated luminosity record of 198 pb^{-1}/day and 1 fb^{-1}/week were recently achieved.

In terms of physics analysis, analyses based on 6 fb^{-1} appeared at the ICHEP conference held in the summer of 2000 at Osaka. Based on data samples of 10 fb^{-1}, four physics papers have been submitted to journals so far. By next summer, a total integrated luminosity of 30 fb^{-1} is expected, and the accelerator luminosity is improving so that there will be lots of room to enjoy B physics in the coming years of the new century.

The author wishes to thank the KEKB accelerator group for the excellent operation. He gratefully acknowledges support of Grant-in-Aid for Encouragement of Young Scientists A12740155 from the Ministry of Education, Science, Sports and Culture and the Japan Society for the Promotion of Science.

REFERENCES

[1] K. Kobayashi, T. Maskawa, *Prog. Theor. Phys.* **49**, 652 (1973).

[2] L. Wolfenstein, *Phys. Rev. Lett.* **51**, 1945 (1983).

[3] K. Abe *et al.* (Belle Collaboration), The Belle Detector, KEK Report 2000-4, to be published in *Nucl. Instrum. Methods Phys. Res.*

[4] D.E. Groom *et al.* (PDG), *Eur. Phys. J.* **C15**, 1 (2000).

[5] A. Abashian *et al.* (Belle Collaboration), *Phys. Rev. Lett.* **86**, 2509 (2001).

[6] M. Bauer, B. Stech, M. Wirbel, *Z. Phys.* **C34**, 103 (1987); M. Wirbel, B. Stech, M. Bauer, *Z. Phys.* **C29**, 637 (1985).

[7] C.S. Jessop *et al.* (CLEO Collaboration), *Phys. Rev. Lett.* **79**, 4533 (1997); T. Affolder *et al.* (CDF Collaboration), *Phys. Rev. Lett.* **85**, 4668 (2000); BaBar Collaboration, SLAC-PUB-8527 (2000).

[8] K. Abe *et al.* (Belle Collaboration), *Phys. Rev. Lett.* **86**, 3228 (2001).

[9] K. Abe *et al.* (Belle Collaboration), `hep-ex/0103042`, submitted to *Phys. Lett.* **B**.

[10] K. Chetrykin, M. Misiak, M. Münz, *Phys. Lett.* **B400**, 206 (1997).

[11] M.S. Alam *et al.* (CLEO Collaboration), *Phys. Rev. Lett.* **84**, 2885 (1995); R. Barate *et al.* (ALEPH Collaboration), *Phys. Lett.* **B429**, 169 (1998).

[12] M. Neubert, *Phys. Rep.* **245**, 259 (1994).